



ELSEVIER

Contents lists available at SciVerse ScienceDirect

Physica B

journal homepage: www.elsevier.com/locate/physb

Design, synthesis and characterization of a linear hydrogen bonded homologous series

C. Kavitha, N. Pongali Sathya Prabu, M.L.N. Madhu Mohan*

Liquid Crystal Research Laboratory (LCRL), Bannari Amman Institute of Technology, Sathyamangalam 638401, India

ARTICLE INFO

Article history:

Received 7 October 2011

Received in revised form

3 December 2011

Accepted 16 December 2011

Available online 23 December 2011

Keywords:

Hydrogen bonded liquid crystals

Smectic X

Re-entrant smectic C

Homeotropic transition

Thermally controlled optical shutter

ABSTRACT

A linear hydrogen bonded liquid crystalline homologous series has been synthesized and characterized. Hydrogen bond is formed between *p*-*n*-dodecyloxy benzoic acid and various *p*-*n*-alkyl benzoic acids whose alkyl chain vary from octyl to ethyl. Synthesized complexes are characterized by FTIR, ¹H NMR and ¹³C NMR studies for inferring the formation of hydrogen bonds. Polarizing Optical Microscopy (POM) and DSC studies reveal various mesophases and their corresponding transition temperatures along with respective enthalpy values. All the seven synthesized complexes exhibit rich liquid crystalline mesomorphism. A new phase namely smectic X has been observed in five of the complexes with a narrow thermal range. This phase has been characterized by optical textural, DSC, tilt angle and helicoidal pitch studies. Smectic X is sandwiched between traditional smectic C and re-entrant smectic C (designated as C_R) phases. Homeotropic transition in nematic phase is observed in all the mesogens and thus these materials can be used as thermally controlled optical shutters. Tilt angle in smectic C, smectic X and smectic C_R phases have been experimentally elucidated for all the mesogens.

© 2011 Elsevier B.V. All rights reserved.

1. Introduction

In the recent years the design of Hydrogen Bonded Liquid Crystals (HBLC) with non-covalent interactions took a new turn in the history of science, which made many researchers to hub their attention towards synthesis of these self assembly systems formed by inter molecular hydrogen bonding. For the formation of liquid crystalline materials through hydrogen bonding interactions, complementarity of the interacting components coupled with the directionability of hydrogen bonds are the main factors contributing to the exhibition of liquid crystallinity. The appropriate shape and stability of the hydrogen bonded complexes are also required. Thus, for non-covalent interactions hydrogen bonding acts as a powerful tool in assembling molecules. The formation of thermotropic liquid crystals with varying characteristics will be based on a categorization of the interacting components according to their structural features (alkyl carbon chain length). Therefore several liquid crystalline materials can be obtained by the interplay of the nature, the number and the location of the recognizable groups in various substrates. It is noticed [1–6] that in hydrogen bonded liquid crystals (HBLC) lower bonding and activation energies showed a profound influence on their thermal properties, viz. clearing points, enthalpies and mesomorphic

phase behavior. Mesogenic properties of HBLC can be tuned easily by changing H-bond donor/ acceptor or percentage of respective molar composition or by changing the length of the alkyl chain. Stable and dynamic molecular complexes can be prepared by simple molecular self assembly processes using such hydrogen bonding. A number of such HBLC have been investigated by Kato et al, which indicates that the mesomorphism results from proper combination of molecular interactions and shape of the molecules. It is inferred [7] that hydrogen bonding has pronounced influence on crystallization and phase behaviors of multi component supra molecular complexes formed by benzoic acids.

The self assembly systems formed between alkyloxy and alkyl carboxylic acids exhibit rich phase polymorphism. It has been earlier reported by us that these self organized systems induce variety of new phenomena like, reentrant phase occurrence [8,9], light modulation [10], optical shuttering action [11–13] and field induced transitions [10,15,16]. The carboxylic acids with other acids are reported [8–16] to form complementary single and multiple hydrogen bonds.

In the present work, we have successfully synthesized a novel series of hydrogen bonded liquid crystal where the inter-molecular hydrogen bonding occurred between *p*-*n*-dodecyloxy benzoic acid and *p*-*n*-alkyl benzoic acids resulting in the formation of seven new HBLCs. Due to the presence of carboxylic acid groups, a stable hydrogen bonded network is formed, whose presence induces the formation of supra molecular structures that exhibit liquid crystalline behavior. Results of homeotropic

* Corresponding author. Tel.: +91 9442437480; fax: +91 4295 223 775.
E-mail address: mln.madhu@gmail.com (M.L.N.M. Mohan).

transition in nematic phase, which can be used as thermally controlled optical shutters along with tilt angle in smectic C, smectic C_R and smectic X phases have been experimentally elucidated for all the mesogens.

2. Material and methods

Optical textural observations were made with a Nikon polarizing microscope (POM) equipped with Nikon digital CCD camera system with 5 mega pixels and 2560 × 1920 pixel resolutions. The liquid crystalline textures were analyzed and stored with the aid of ACT-2U imaging software system. The temperature control of the liquid crystal cell was equipped by Instec HCS402-STC 200 temperature controller (Instec, USA) to a temperature resolution of ± 0.1 °C. This unit was interfaced to computer by IEEE-STC 200 to control and monitor the temperature. The liquid crystal sample was filled by capillary action in its isotropic state into a commercially available (Instec, USA) polyamide buffed cell with 4 μm spacer. Optical extinction technique [16] was used for determination of tilt angle. Transition temperatures and corresponding enthalpy values were obtained by DSC (Shimadzu DSC-60, Japan). FTIR spectra were recorded (ABB FTIR MB3000) and analyzed with the MB3000 software. The p-n-dodecyloxy benzoic acid (12BAO) and p-n-alkyl benzoic acids (nBA, where n=2–8) were supplied by Sigma Aldrich, (Germany) and all the solvents were of HPLC grade.

2.1. Synthesis of HBLC

All the inter-hydrogen bonded complexes examined in the present study are prepared by mixing in 1:1 molar ratio dodecyloxy benzoic acid with various alkyl benzoic acids in DMF and reprecipitating after the evaporation as described in the reported

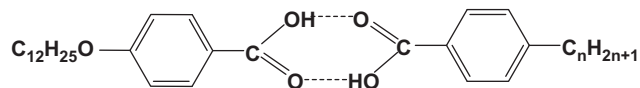


Fig. 1. Molecular structure of 12BAO + nBA homologous series.

literature [1,2,4]. Molecular structure of the present homologous series of p-n-dodecyloxy benzoic acid (12BAO) with p-n-alkyl benzoic acids (nBA, where n=2–8) is depicted in the Fig. 1 where n represents the alkyl carbon number.

3. Results and discussion

All the hydrogen bonded complexes isolated under the present investigation are white crystalline solids and are stable at room temperature (30 °C). They are insoluble in water and sparingly soluble in common organic solvents such as methanol, ethanol, benzene and dichloro methane. However, they show a high degree of solubility in coordinating solvents like dimethyl sulfoxide (DMSO), dimethyl formamide (DMF) and pyridine. All these mesogens melt at specific temperatures below ~82 °C (Table 1). They show high thermal and chemical stability when subjected to repeated thermal scans performed during Polarizing Optical Microscopy (POM) and DSC studies.

3.1. Phase identification

The observed phase variants, transition temperatures and corresponding enthalpy values obtained by DSC in the cooling and heating cycles for the 12BAO + nBA complexes are presented in Table 1. These data are in concurrence with POM data.

3.2. 12BAO + nBA homologous series

The mesogens of the p-n-dodecyloxy benzoic acid (12BAO) with p-n-alkyl benzoic acids (nBA, where n=2–8) designated as 12BAO + nBA homologous series are found to exhibit characteristic textures [17], viz., nematic (N) (threaded texture, Plate 1), homeotropic region of nematic (N_h), (Plate 2), smectic C (schlieren texture, Plate 3) smectic X (worm like texture, Plate 4) and reentrant smectic C designated as smectic C_R (broken focal conic texture, Plate 5). The general phase sequence of various homologs of 12BAO + nBA series in cooling and heating run can be shown as

Iso ⇌ N → N_h → N ⇌ Sm C → Sm X → Sm C_R ⇌ Crystal (12BAO + 8BA)

Table 1
Transition temperatures and enthalpy values obtained by various techniques of 12BAO + nBA homologous series.

Complex	Phase Variance	Techniques	Melt	N	Homeotropic (N _h)	N _h	C	X	C _R	Crystal
12BAO + 8BA	NN _h NCXC _R	DSC (h)	57.0 (20.89)	125.9 (4.62)	*	⊕	100.0 (1.35)	*	*	
		DSC (c)		122.0 (4.53)	*	111.7 (0.13)	97.3 (1.26)	*	*	44.5 (16.75)
		POM		122.7	116.3		112.3	97.8	91.6	90.5
12BAO + 7BA	NN _h NCXC _R	DSC (h)	62.3 (32.46)	⊕	*		129.3 (7.92)	*	*	91.8 (0.82)
		DSC (c)		139.9 (0.49)	*	127.3 (7.5)	*	*	91.7 (0.96)	47.9 (37.67)
		POM		140.6	129.0		127.8	119.3	93.2	92.0
12BAO + 6BA	NN _h NCXC _R	DSC (h)	60.4 (17.46)	129.5 (2.87)		*	*	101.1 (0.09)	*	
		DSC (c)		130.1 (0.19)	120.3 (2.86)	*	*	*	*	51.3 (15.51)
		POM		129.6	121.1	115.6	112.2	101.6	100.5	51.8
12BAO + 5BA	NN _h CXC _R	DSC (h)	64.2 (33.59)	129.3 (4.77)	⊕		109.1 (0.08)	*	*	56.9 (22.72)
		DSC (c)		129.8 (0.36)	125.9 (4.32)		109.7	99.7	99.0	57.4
		POM		130.5	126.7		*	*	*	
12BAO + 4BA	NN _h CXC _R	DSC (h)	61.6 (16.56)	127.2 (3.47)	⊕		*	*	*	54.2 (11.07)
		DSC (c)		128.8 (0.34)	123.6 (3.3)		*	*	*	54.9
		POM		129.7	124.1		119.3	97.6	97.0	
12BAO + 3BA	NN _i C	DSC (h)	82.1 (13.26)	129.0 (1.45)	*		*	*	*	69.9 (13.63)
		DSC (c)		126.3 (2.45)	*		*	*	*	70.2
		POM		126.9	106.2		92.1			
12BAO + 2BA	NN _i C	DSC (h)	64.8 (27.88)	128.9 (3.89)	*		*	*	*	53.9 (25.4)
		DSC (c)		126.2 (3.82)	*		*	*	*	54.2
		POM		126.8	112.1		110.5			

Temperatures in °C while enthalpy in J/g is given in parenthesis.

* not resolved.

⊕ monotropic transition.

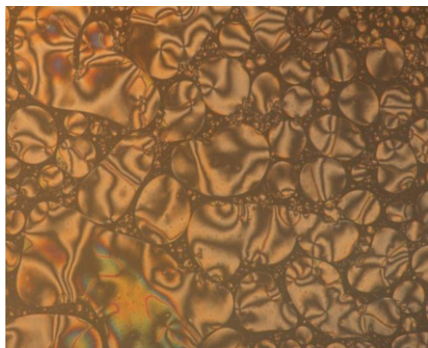


Plate 1. Nematic schlieren texture of 12BAO+8BA complex.



Plate 4. Fully grown smectic X phase observed in 12BAO+8BA complex.



Plate 2. Texture of homeotropic region (N_h) of nematic observed in 12BAO+8BA complex.

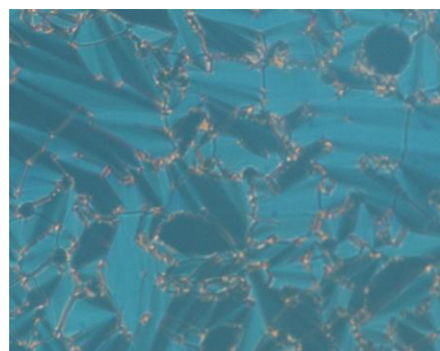


Plate 5. Broken focal conic texture of smectic C_R in 12BAO+8BA complex.

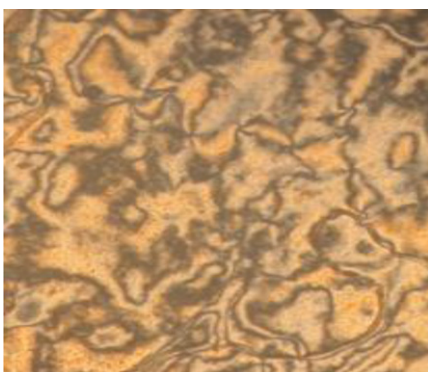


Plate 3. Schlieren texture of smectic C in 12BAO+8BA complex.

$\text{Iso} \rightarrow \text{N} \rightarrow N_h \rightleftharpoons \text{N} \rightarrow \text{Sm C} \rightarrow \text{Sm X} \rightleftharpoons \text{Sm } C_R \rightleftharpoons \text{Crystal (12BAO+7BA)}$

$\text{Iso} \rightleftharpoons \text{N} \rightarrow N_h \rightarrow \text{N} \rightarrow \text{Sm C} \rightarrow \text{Sm X} \rightarrow \text{Sm } C_R \rightleftharpoons \text{Crystal (12BAO+6BA)}$

$\text{Iso} \rightleftharpoons \text{N} \rightarrow N_h \rightarrow \text{Sm C} \rightarrow \text{Sm X} \rightarrow \text{Sm } C_R \rightleftharpoons \text{Crystal (12BAO+5 and 4 BA)}$

$\text{Iso} \rightleftharpoons \text{N} \rightarrow N_h \rightarrow \text{Sm C} \rightleftharpoons \text{Crystal (12BAO+3 and 2 BA)}$.

Monotropic and enantiotropic transitions are depicted as single and double arrows, respectively.

3.3. Spectroscopic studies

3.3.1. Fourier Transform Infrared Spectroscopy (FTIR)

IR spectra of all the HBLC complexes are recorded in the solid state (KBr) at room temperature. As a representative case, Fig. 2a illustrates the FTIR spectra of 12BAO+8BA in solid state at room temperature. It can be noticed that the O–H stretching band

involving H-bond dimer and the Fermi resonances in the precursor (Fig. 2a (i)) are observed at 2554 cm^{-1} and 1913 cm^{-1} , respectively [18,19]. Once the complexation is complete the O–H stretching band and its Fermi resonance appear at 2561 cm^{-1} and 1906 cm^{-1} , respectively, and no peak due to dimerization of benzoic acid moieties is seen. Moreover, the carbonyl band observed at 1690 cm^{-1} of the pre-cursors shifts to 1682 cm^{-1} after complexation due to formation of hydrogen bond between carboxylic acids. These results support the hydrogen bonded network structures have been obtained by the dominant formation of the thermodynamically favored inter-molecular hydrogen bonds between the individual components [19]. These results concur with the reported results on H-bond mesogens [20].

3.3.2. ^1H NMR studies

The proposed molecular structure is verified by the ^1H NMR studies. The ^1H NMR spectra are recorded for all the synthesized complexes under present investigation. As a representative case, the spectrum of 12BAO+4BA is discussed. ^1H NMR spectrum of the complex is recorded in CDCl_3 with TMS (tetramethylsilane) as the internal standard. The following chemical shifts were observed in the spectrum:

- Broad resonance signals are observed approximately in the range of 0.5–2.8 ppm for the methylene group. In the 12BAO+4BA complex these signals are observed between 2.685 and 0.878 ppm, which has been attributed to the existence of the backbone methylene.
- Sets of multiplets between 7.963–7.933 ppm, 7.675 ppm and 7.255–7.229 ppm and 6.916–6.887 are assigned to aromatic protons.
- The existence of the methoxy proton unit resonance showed a signal at 4.009 ppm.

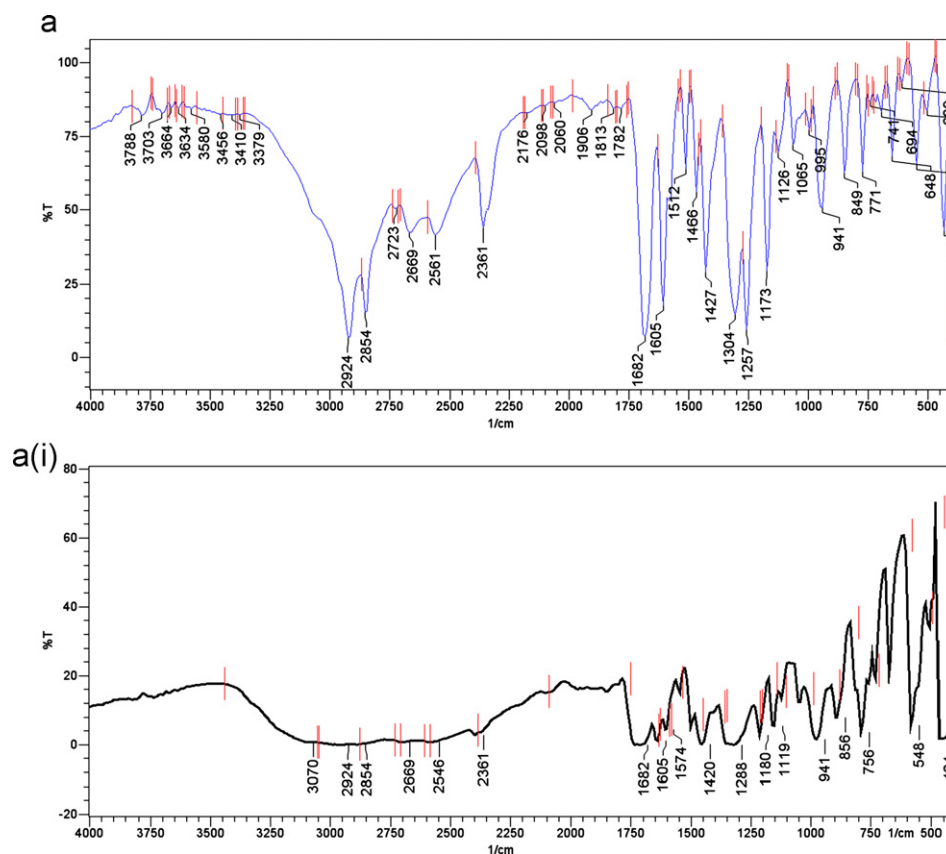


Fig. 2. (a) FTIR spectra of 12BAO+8BA complex. (a(i)) FTIR spectra of pure 8BA.

(d) The non appearance of a peak at 11.0–12.0 ppm for the carboxylic acid hydrogen in the ^1H NMR spectra also stands a proof for the involvement of that hydrogen in inter-molecular hydrogen bonding.

The shifts obtained through ^1H NMR study are found in accordance to the proposed molecular structure.

3.3.3. ^{13}C NMR studies

The projected organic molecular structure of the complex is verified through ^{13}C NMR study. The ^{13}C NMR spectra are recorded for all the synthesized complexes under present investigation. As a representative case, the spectrum 12BAO+4BA is discussed. This study infers the information regarding the number of non equivalent carbons and also to identify the types of carbon atoms (methyl, methylene, aromatic, carbonyl and so on). Hence the carbon skeleton of the organic molecule can be deduced completely with the aid of the ^{13}C NMR study.

^{13}C NMR spectrum of the complex was recorded in CDCl_3 with TMS (tetramethylsilane) as the internal standard. AS a representative case, the spectrum of 12BAO+4BA is elaborately discussed. The recorded spectrum includes the following chemical shifts:

- Broad resonance magnetic signals are observed approximately in the range of 34.493–15.882 ppm, which contributes to the methylene carbon.
- A multiplet shift achieved at 7.825–7.607 ppm is assigned to the methyl carbon.
- The existence of the alkyloxy carbon in the proposed molecule is confirmed by the shift observed at 72.095–61.812 ppm.
- Multiple resonance magnetic signals obtained at 125.332–107.678 ppm are due to the benzene carbon.

(e) The sharp signal obtained at 156.410 ppm is attributed to the oxy-carboxylic acid carbon.

(f) The sharp signal obtained at 161.689 ppm is attributed to the carboxylic acid carbon.

Thus the proposed structure of the organic molecule is further confirmed with ^{13}C NMR studies.

3.4. DSC studies

DSC thermograms are recorded in heating and cooling cycle. The sample is heated with a scan rate of $10^\circ\text{C}/\text{min}$ and held at its isotropic temperature for 2 min so as to attain thermal stability. The cooling run is performed with the same scan rate of $10^\circ\text{C}/\text{min}$. The respective equilibrium transition temperatures and corresponding enthalpy values of the mesogens of the homologous series are listed separately in Table 1. POM studies also concur with the DSC transition temperatures. As a representative case the DSC thermogram including both the heating and cooling cycles are depicted in Fig. 3. A graph designated as Fig. 3 depicts the endothermic and exothermic DSC thermogram of 12BAO+8BA complex. It is plotted for the DSC heating and cooling thermograms by assigning the temperature variation along X-axis and the corresponding enthalpy value (ΔH) along Y-axis.

3.5. Phase diagram of pure *p*-*n*-alkyloxy benzoic acid

The phase diagram of pure 12BAO is reported [21,22] to compose of two phases namely, nematic and smectic C.

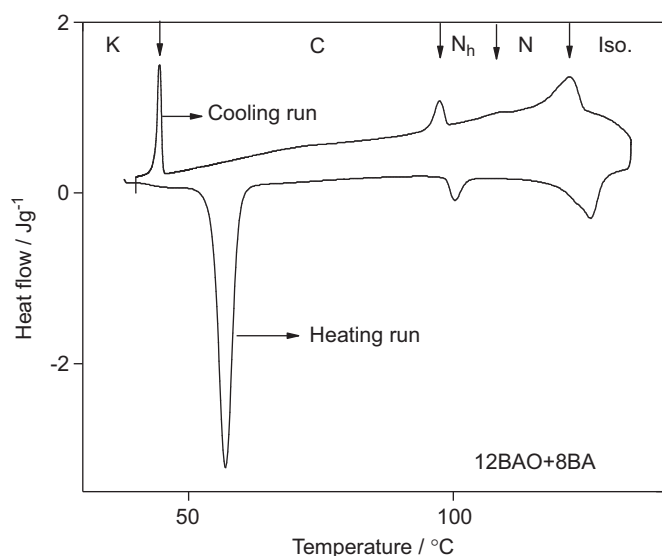


Fig. 3. DSC thermograms obtained in cooling cycle of 12BAO + *n*BA complexes.

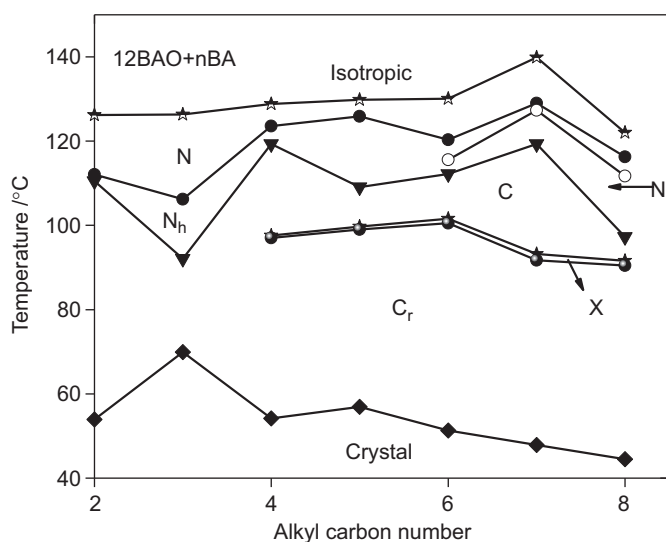


Fig. 4. Phase diagram of 12BAO + *n*BA homologous series.

3.5.1. Phase diagram of 12BAO + *n*BA

Phase diagram of *p*-*n*-dodecyloxy benzoic acid and *p*-*n*-alkyl benzoic acids (12BAO + *n*BA) homologs series are depicted in Fig. 4. The following points can be elucidated from Fig. 4:

- The 12BAO + *n*BA hydrogen bonded homologous series exhibits nematic as orthogonal phase while smectic C, smectic X and smectic C_R as tilted phases.
- The nematic phase along with homeotropic region of nematic and smectic C are prevailing throughout the homologs of the series.
- The smectic X phase is induced only from butyl to octyl benzoic acids quenching the thermal range of smectic C. Further smectic X is sandwiched between smectic C and re-entrant smectic C phases.
- The thermal span of nematic and re-entrant C phase are observed to be invariant with increasing alkyl chain length.
- The mesogenic thermal span is found to increase with increasing alkyl chain length.
- An interesting observation in the present homologs series is the absence of odd–even effect at isotropic to nematic and

smectic C_R to crystal interfaces. Moreover there is no appreciable change in isotropic temperatures.

- The occurrence of smectic X phase is attributed to the *l/d* ratio of the homologs series. The lower homologs failed to have a threshold value of *l/d* ratio, which in turn reflects in the absence of smectic X phase.
- A gradual decrease in the crystallization temperatures is observed from pentyl benzoic acid to ethyl benzoic acid.

4. Optical tilt angle measurement

The optical tilt angle has been experimentally measured by optical extinction method [16] in smectic C and smectic C_R phases of all the members of the present 12BAO + *n*BA homologous series. Figs. 5–10 depict such variation of optical tilt angle with temperature for 12BAO + *n*BA (where *n* = 2–8) series. In Figs. 5–10 the theoretical fit obtained from the Mean field theory is denoted by the solid line. It is observed from the Figs. 5–10, that the tilt angle increases with decreasing temperature and attains a

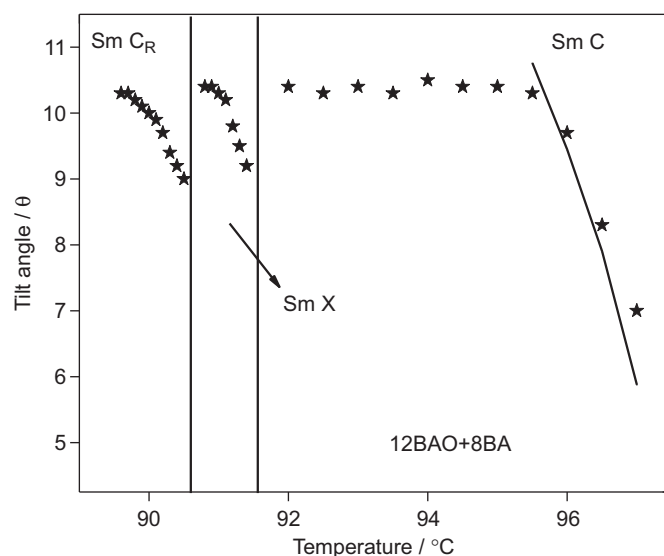


Fig. 5. Optical tilt angle measurement in smectic C, X and C_R phases of 12BAO + 8BA complex.

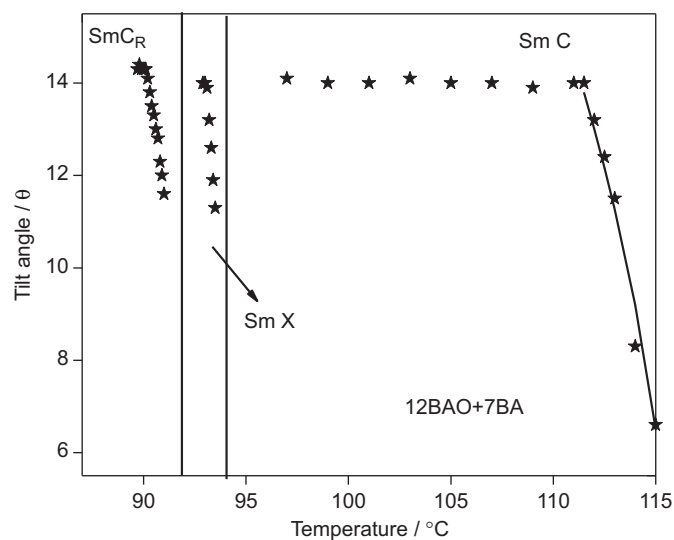


Fig. 6. Optical tilt angle measurement in smectic C, X and C_R phases of 12BAO + 7BA complex.

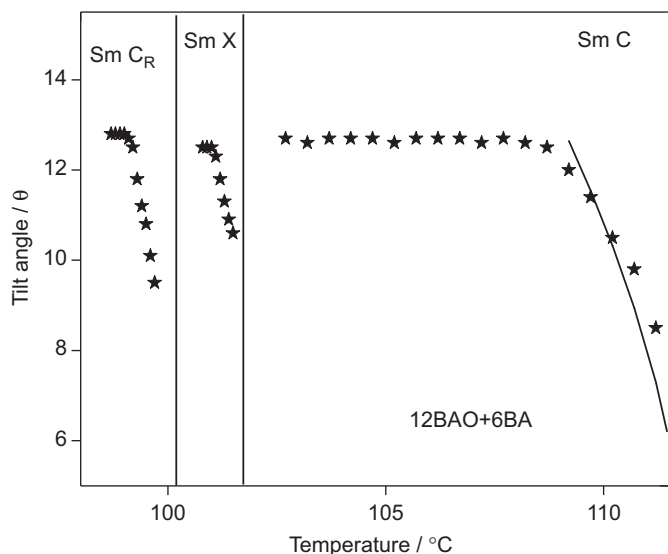


Fig. 7. Optical tilt angle measurement in smectic C, X and C_R phases of 12BAO+6BA complex.

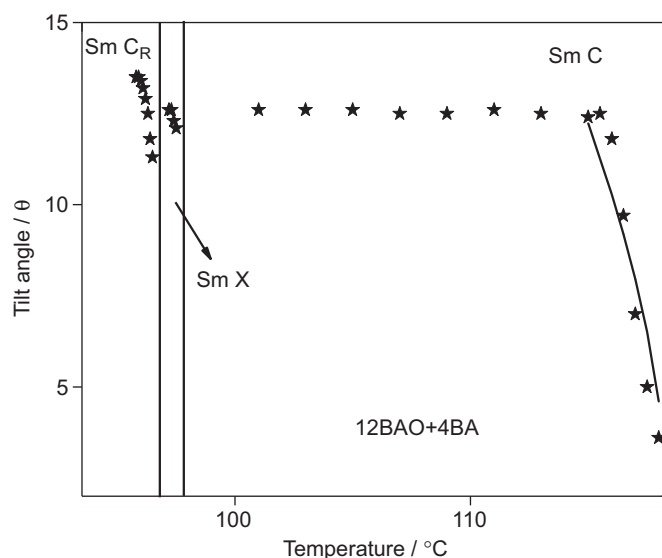


Fig. 9. Optical tilt angle measurement in smectic C, X and C_R phases of 12BAO+4BA complex.

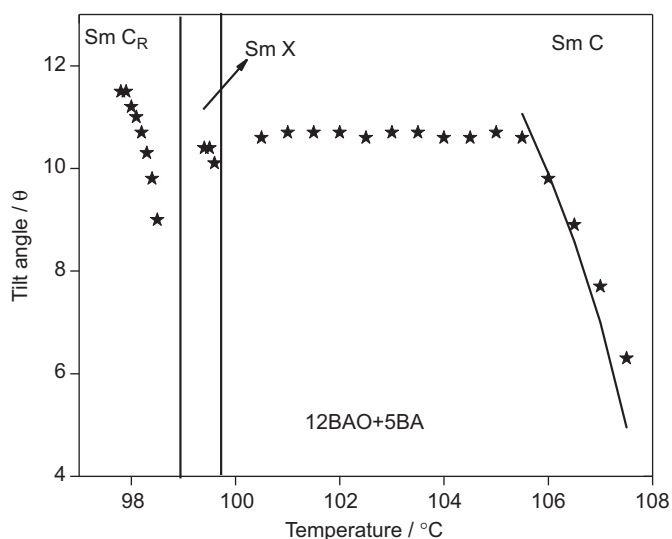


Fig. 8. Optical tilt angle measurement in smectic C, X and C_R phases of 12BAO+5BA complex.

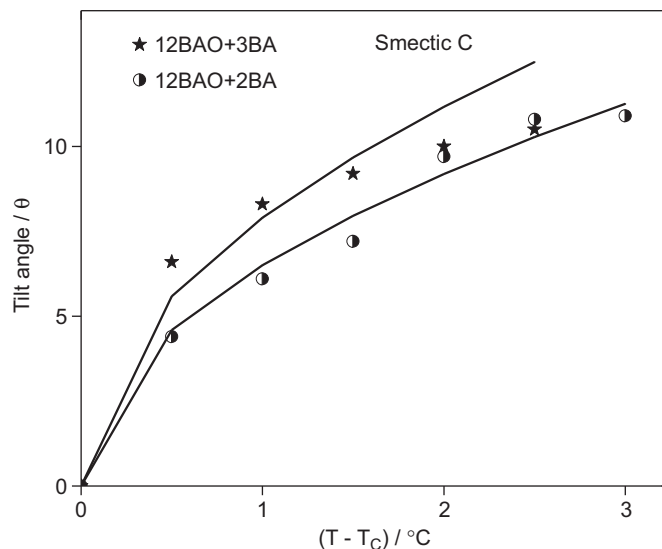


Fig. 10. Optical tilt angle measurement in smectic C phase of 12BAO+nBA complexes (where $n=3$ and 2).

saturation value. These large magnitudes of the tilt angle are attributed to the direction of the soft covalent hydrogen bond interaction, which spreads along molecular long axis with finite inclination [23].

Tilt angle is a primary order parameter [24] and the temperature variation is estimated by fitting the observed data of $\theta(T)$ to the relation

$$\theta(T) \propto (T_C - T)^\beta \quad (1)$$

The critical exponent β value estimated by fitting the data of $\theta(T)$ to the above Eq. (1) is found to be 0.50 to agree with the Mean field prediction [25,26]. The solid lines in the Figs. 5–10 depict the fitted data for various mesogens. Further, the agreement of magnitude of β (0.5) with the Mean field value (0.5) infers the long-range interaction of transverse dipole moment for the stabilization of tilted smectic C and C_R phases.

4.1. Optical tilt angle measurements in smectic C, X and C_R phases

4.1.1. Tilt angle measurement in 12BAO+8BA complex

The onset of the smectic C phase is observed at 97.3 °C. As the temperature is decreased, the optical tilt angle value increases from 7° to 10.4° and attains a saturation value at 95 °C as can be noticed from Fig. 5. The optical tilt angle has been fitted to power law and the solid line indicates the fitted data. Further the magnitude of β (0.5) is observed to be in concurrence with the Mean field theory predicted value.

On further decrease of temperature the smectic C phase of 12BAO+8BA paves way for a new phase namely smectic X at 91.6 °C whose thermal range is observed to be very narrow (~ 1.1 °C). The magnitude of tilt angle increases with decreasing temperature and attains a saturated value. The tilt angle magnitude varies from 9° to 10.5° in this smectic X phase and as the phase is fully grown the magnitude of the tilt angle saturates at 10.5°.

On further decrease of temperature to 90.5 °C the re-entrant smectic C_R is observed. The magnitude of the tilt angle is 8.7° at 90.5 °C and increases to 10.5° before attaining a saturated value at 89.5 °C.

In all these tilted phases viz., smectic X and smectic C_R phase, the magnitude of the saturated optical tilt angle measured is approximately equal to the saturated tilt angle value observed in smectic C phase.

4.1.2. Tilt angle measurement in 12BAO+7BA complex

In this hydrogen bonded complex the smectic C phase originates at 119.3 °C. The variation of tilt angle with temperature is depicted in Fig. 6. In smectic C phase with decreasing temperature the optical tilt angle value increases from 6.6° and attains a saturation value of 14° at a temperature of 111 °C. The fitted tilt value obtained from Eq. (1) is shown as a solid line in Fig. 6. The critical exponent β value estimated by fitting the data of $\theta(T)$ is observed to follow the Mean field theory predicted value.

At 93.2 °C a new phase designated as smectic X with a narrow temperature range (~ 1.5 °C) is observed. As the temperature decreased in small steps the magnitude of the tilt angle varied from 11° to 14° in this phase before attaining a saturated value of 14°.

On further decrease of temperature re-entrant smectic phase designated as C_R is observed at 91.7 °C. The magnitude of the tilt angle is observed to increase with the decrement of temperature. As the phase is fully grown the magnitude of the tilt angle saturates to a value of 14.1° at 89.8 °C.

In the three tilted phases viz. smectic C, smectic X and smectic C_R phases, the magnitude of the optical tilt angle is almost the same.

4.1.3. Tilt angle measurement in 12BAO+6BA complex

The onset of smectic C phase in 12BAO+6BA is observed at 112.2 °C. As the temperature is decreased the magnitude of the tilt angle increases and attains a saturated value. The variation of temperature dependence of tilt angle is depicted in Fig. 7. The magnitude of the optical tilt angle value varied between 7.1° and 12.7° with decreasing temperature and attains a saturation value of 12.7° at a temperature of 107.7 °C. The theoretical tilt value obtained from Eq. (1) is shown as a solid line in Fig. 7. The critical exponent β value estimated by fitting the data of $\theta(T)$ is observed to follow the Mean field theory predicted value.

As the temperature is further decreased at 101.6 °C a new phase designated as smectic X with a very narrow (~ 1.1 °C) thermal range have been observed. In this phase as the temperature is decreased in small steps, the magnitude of the tilt angle increases from 11° to 12.7° and saturates as shown in Fig. 6. The saturated magnitude of the tilt angle 12.7° is observed at 100.6 °C.

On further decrement of temperature to 100.5 °C a re-entrant smectic phase designated as C_R is observed. The magnitude of the tilt angle in this phase varies between 9° and 12.8° with temperature. The saturated value of 12.8° is observed at 98.5 °C.

In all the three tilted phases viz. smectic C, smectic X and smectic C_R phases, the saturated magnitude of the optical tilt angle is observed to be almost invariant as can be seen from Fig. 7.

4.1.4. Tilt angle measurement in 12BAO+5BA complex

In the 12BAO+5BA complex the onset of smectic C is observed at 109.1 °C. Fig. 8 illustrates the variation of optical tilt angle value with temperature. From the Fig. 8 it can be observed that as temperature is decreased the magnitude of the tilt angle increases initially and attains a saturated value. The magnitude of the tilt angle saturates to 10.6° at 106 °C. The theoretical tilt values obtained from Eq. (1) are shown as a solid line in Fig. 8. The

critical exponent β value estimated by fitting the data of $\theta(T)$ is observed to follow the Mean field theory predicted value.

On decreasing the temperature in small steps of 0.1 °C at 99.7 °C a new phase designated as smectic X with very narrow thermal range (~ 0.7 °C) is observed. The saturated magnitude of the tilt angle is observed to be 10.6° at 99.6 °C.

On further decreasing the temperature to 99.0 °C a new phase designated as reentrant smectic C_R phase is observed. The saturated magnitude of the tilt angle is observed to be 11.6° at 98.1 °C.

In all the three tilted phases viz. smectic C, smectic X and smectic C_R phases, the saturated magnitude of the optical tilt angle is observed to be almost invariant as can be seen from Fig. 8.

4.1.5. Tilt angle measurement in 12BAO+4BA complex

The onset of smectic C is observed at 119.3 °C in 12BAO+4BA complex. Fig. 9 illustrates the variation of optical tilt angle value with temperature. From Fig. 9 it can be observed that the magnitude of the tilt angle increases with decrement in temperature. The magnitude of the tilt angle saturates to 12.5° at 115.5 °C. The theoretical tilt value obtained from Eq. (1) is shown as a solid line in Fig. 9. The critical exponent β value estimated by fitting the data of $\theta(T)$ is observed to follow the Mean field theory predicted value.

As the temperature is further decreased, at 97.6 °C a new phase designated as smectic X with a very narrow thermal range (~ 0.6 °C) is observed. In this phase, as the temperature is decreased in small steps of 0.1 °C, the magnitude of the tilt angle increases and gets saturated as shown in Fig. 9. The magnitude of the tilt angle saturates to 12.5° at 97.3 °C.

On further decrement of temperature to 97.0 °C a re-entrant smectic phase designated as C_R is observed. The magnitude of the tilt angle in this phase varies between 11.3° and 13.5° with temperature. The saturated value of 13.5° is observed at 95.8 °C.

In all the three tilted phases viz. smectic C, smectic X and smectic C_R phases, the saturated magnitude of the optical tilt angle is observed to be almost invariant as can be seen from Fig. 9.

4.1.6. Tilt angle measurement in 12BAO+3BA complex

In this hydrogen bonded complex the smectic C phase originates at 92.1 °C. The variation of tilt angle with temperature is depicted in Fig. 10. In smectic C phase, with decrement in temperature the optical tilt angle value increases from 4.4° and attains a saturation value of 10.9° at a temperature of 94.6 °C. The fitted tilt value obtained from Eq. (1) is shown as a solid line in Fig. 6. The critical exponent β value estimated by fitting the data of $\theta(T)$ is observed to follow the Mean field theory predicted value. In this lower homolog smectic X and smectic C_R phases have been quenched.

4.1.7. Tilt angle measurement in 12BAO+2BA complex

The onset of the smectic C phase is observed at 110.5 °C. As the temperature is decreased, the optical tilt angle value increases from 6.6° to 10.5° and attains a saturation value. The optical tilt angle has been fitted to power law and the solid line indicates the fitted data. Further the magnitude of β (0.5) is observed to be in concurrence with the Mean field theory predicted value. Like 12BAO+3BA complex in this lower homolog also the smectic X and smectic C_R phases have been quenched. The variation of tilt angle with temperature is depicted in Fig. 10.

4.2. Possible reasons for the occurrence of re-entrant smectic C_R

The appearance of finger print texture with decrease of temperature (in $n=4-8$ as sandwiched between SmC and Sm C_R)

can be explained on the premise of a frustration (i.e., deformation or disruption) of the long range tilt (grown in the higher temperature SmC phase) ordering. With the decrease of temperature, the molecules of SmC phase come closer. As such, the separation of dipolar pair decreases to increase the repulsion, which leads to the loss of stability of the high temperature C-phase. However, if one molecule in n th smectic layer re-adjusts to slide onto the adjacent layer, the repulsive interaction can be reduced. Thus, the spoilage of long range layered tilt order (especially in homologs, viz., for $n=4-8$) leads to the protrusion of end chains into the adjacent layers. Further, the steric factors (as manifested by the protruding end chains) become prevalent with decreasing temperature. A broken tilt order with decreasing temperature leads to the formation of domains with features of SmC. They are familiarized with cybotactic nematic domains. However, further decrease of temperature naturally leads to the growth of some sort of correlation among these domains. Thus, the growth of correlation among tilted smectic domains leads for their coalescing to result in the growth of smectic C_R phase.

5. Characterization of smectic X phase

Smectic X phase, which has been identified in five complexes namely 12BAO+8BA, 12BAO+7BA, 12BAO+6BA, 12BAO+5BA and 12BAO+4BA is characterized by textural studies. In all the above complexes, smectic X is sandwiched between traditional smectic C and reentrant smectic C_R phases. This serves as one of the strongest evidence to identify this new phase smectic X as smectic ordering.

5.1. Textural study of smectic X phase

The hydrogen bonded complexes from 12BAO+8BA to 12BAO+4BA, on cooling from isotropic phase nematic droplets are observed. On further cooling, a worm like texture is observed, which is designated as smectic X and depicted as Plate 4. The thermal width of this phase is very narrow ($< 1^\circ\text{C}$) and the fully grown phase is shown as Plate 4. The striations in the worm like texture are manifestation of the presence of helicoidal structure. This phase has been characterized in earlier hydrogen bonded liquid crystals [16] by us. With further decrement of temperature this phase paves way for broken focal conic texture of smectic C_R phase as shown in Plate 5. Interestingly, this smectic X phase is observed to be monotropic. The nematic to smectic C transition is observed to be second order and hence could not be resolved in the DSC thermograms, similarly smectic X to smectic C is also observed to be second order transition.

5.2. DSC studies of smectic X phase

Interestingly the smectic X phase exhibits monotropic transition in the performed thermal scans hence it is observed only in the heating run of the 12BAO+6BA complex. In the other complexes exhibiting this phase it is unresolved although the thermal scan is performed at a scan rate of $5^\circ\text{C}/\text{min}$. The enthalpy value of this phase transition clearly indicates that it is a weak second order transition.

5.3. Helical pitch measurement

In the present work, the helical pitch is measured by diffraction of He-Ne red laser light on liquid crystal sample filled in a commercially available (Instec) buffed conducting cell. This method can be used for measurement of the helical pitch of short length. Helicoidal pitch of all the complexes has been

measured. As a representative case the temperature variation of 12BAO+8BA helicoidal structure is discussed.

The deformation of the helicoidal structure has been experimentally analyzed by varying the temperature. As the temperature is decremented in small steps the variation of the helix is noted at each step. The variation of normalized helix with temperature is depicted as Fig. 11. The unwinding of the helix with temperature in smectic X phase indicates that this phase is not only tilted but also possesses helicoidal structure. Liquid crystal in the smectic X phase acts as a grating and a diffraction pattern is thus observed on the screen. The first order diffraction pattern observed is recorded and depicted as Plate 6.

5.4. Ordering in smectic X

Smectic X phase is sandwiched between traditional smectic C and re-entrant smectic C referred as smectic C_R . The molecular orientation in various phases is depicted in Fig. 12. From Fig. 12 it can be seen that the flipping of the molecules is taking place. The high magnitude of the helix in smectic X phase compared to its preceding and succeeding phases stands as a token of evidence for the molecular re-orientation. Thermo dynamical conditions favor this smectic X phase with narrow thermal span where the flipping of the molecules occur.

POM, optical tilt angle and helicoidal structural studies enable this phase to be a smectic ordering. This argument is valid with

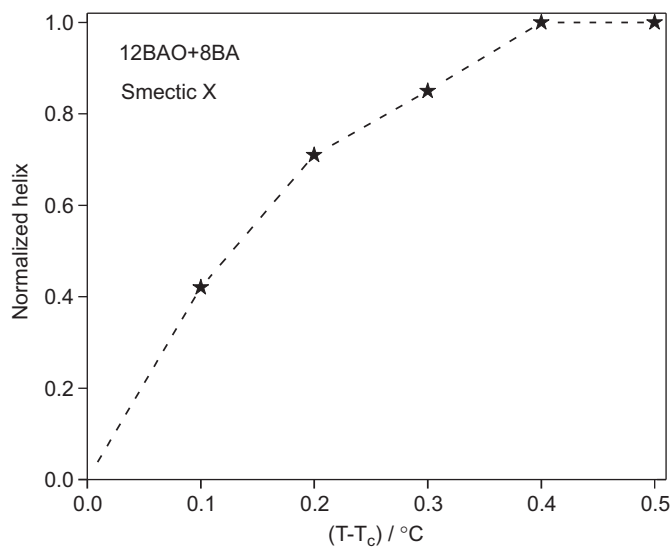


Fig. 11. Temperature variation of helicoidal structure of 12BAO+8BA complex.



Plate 6. Diffraction pattern corresponding to helicoidal measurement of 12BAO+8BA complex.

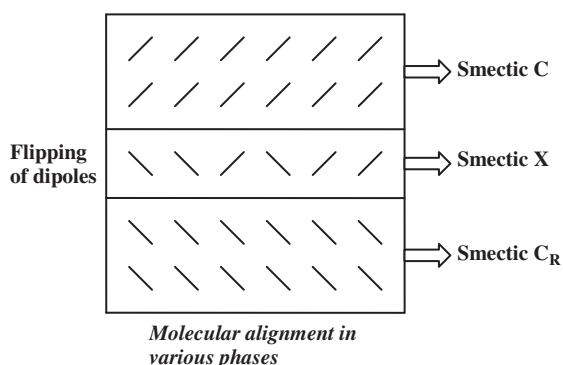


Fig. 12. Molecular orientation in various phases.

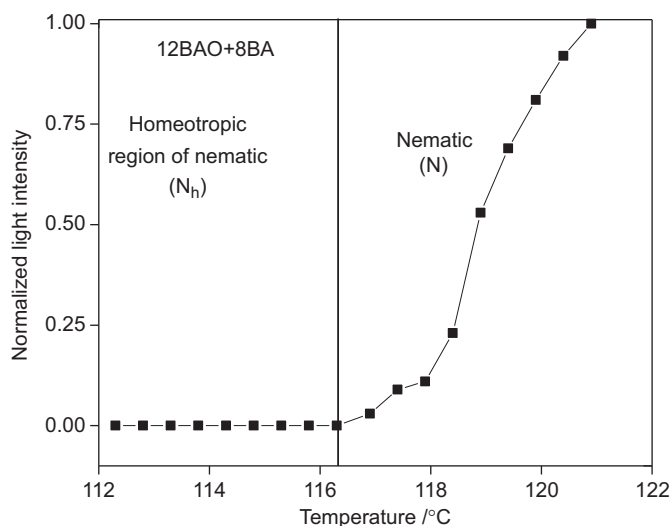


Fig. 13. Temperature variation of intensity of light in 12BAO+8BA complex.

yet another evidence where, smectic X is sandwiched between two smectic orderings.

6. Thermally tuned optical shuttering action

All the seven hydrogen bonded complexes of 12BAO+*n*BA exhibit nematic to homeotropic transition and the relevant transition temperatures of various homologous are tabulated in Table 1. In all the seven homologs studied, the nematic phase is manifested by a threaded nematic texture as shown in Plate 1.

As a representative case, thermally tuned optical shuttering action in 12BAO+8BA complex is discussed. The onset of the nematic phase is observed at 122.0 °C with threaded nematic texture. The intensity of the plane polarized light pertaining to the nematic texture under the crossed polarizers is measured with a photo diode TSL 252 at various predetermined temperatures. With the decrement of the temperature in small steps of 0.5 °C the onset of homeotropic region of nematic phase designated as N_h is noticed, which is shown as Plate 2. The intensity of the plane polarized light in the nematic, and homeotropic nematic phase are measured. Fig. 13 illustrates the variation of normalized light intensity with the temperature. As the nematic to homeotropic region of nematic occurs, the plane polarized light intensity gradually decreases and in homeotropic region of

nematic, the extinction of light intensity is noticed. The light shuttering action in the entire thermal span of homeotropic region of nematic phase can be clearly seen from Fig. 13. Thus all these seven homologous in homeotropic region of nematic phase can be thermally tuned for optically shuttering action, which can be exploited for commercial applications.

7. Conclusions

- (1) A novel series of HBLC is synthesized and characterized by various techniques.
- (2) Typical smectic phases like smectic X and smectic C_R have been observed in certain complexes.
- (3) All the phases observed are confirmed by the textural observation, optical tilt angle measurement and DSC studies.
- (4) The observation of homeotropic region in nematic phases observed in all the complexes enables the mesogens to be used as a thermally tuned optical shutter.
- (5) Optical tilt angles for the various tilted phases like smectic C, smectic X and smectic C_R are measured and compared.

Acknowledgments

The divine blessings of almighty Bannari Amman and the infrastructural support rendered by the Bannari Amman Institute of Technology are gratefully acknowledged.

References

- [1] T. Kato, J.M.J. Frechet, *J. Am. Chem. Soc.* 111 (1989) 8533.
- [2] T. Kato, J.M.J. Frechet, *Macromol. Symp.* 95 (1995) 311.
- [3] T. Kato, *Supramol. Sci.* 3 (1996) 53.
- [4] T. Kato, J.M.J. Frechet, *Macromolecules* 22 (1989) 3818.
- [5] U. Kumar, T. Kato, J.M.J. Frechet, *J. Am. Chem. Soc.* 114 (1992) 6630.
- [6] H. Kihara, T. Kato, S. Ujiiie, T. Uryu, U. Kumar, J.M.J. Frechet, D.W. Bruce, D.J. Price, *Liq. Cryst.* 21 (1996) 25.
- [7] X. Lu, C. He, A.C. Griffins, *Macromolecules* (2003) 5195.
- [8] V.N. Vijayakumar, K. Murugadass, M.L.N. Madhu Mohan, *Mol. Cryst. Liq. Cryst.* 517 (2010) 43.
- [9] T. Chitravel, M.L.N. Madhu Mohan, *Mol. Cryst. Liq. Cryst.* 524 (2010) 131.
- [10] V.N. Vijayakumar, M.L.N. Madhu Mohan, *Mol. Cryst. Liq. Cryst.* 517 (2010) 113.
- [11] V.N. Vijayakumar, M.L.N. Madhu Mohan, *J. Opt. Electron. Adv. Mater.* 11 (8) (2009) 1139.
- [12] N. Pongali Sathya Prabu, V.N. Vijayakumar, M.L.N. Madhu Mohan, *Mol. Cryst. Liq. Cryst.* 548 (2011) 142.
- [13] V.N. Vijayakumar, M.L.N. Madhu Mohan, *Solid State Sci.* 12 (4) (2010) 142.
- [14] V.N. Vijayakumar, M.L.N. Madhu Mohan, *Braz. J. Phys.* 39 (4) (2009) 677.
- [15] N. Pongali Sathya Prabu, V.N. Vijayakumar, M.L.N. Madhu Mohan, *Mol. Cryst. Liq. Cryst.* 548 (2011) 73.
- [16] V.N. Vijayakumar, M.L.N. Madhu Mohan, *Solid State Commun.* 149 (2009) 2090.
- [17] G.W. Gray, J.W.G. Goodby, *Smectic Liquid Crystals: Textures and Structures*, Leonard Hill, London, 1984.
- [18] T. Kato, C. Jin, F. Kaneughi, T. Uryu, *Bull. Chem. Soc. Jpn.* 66 (1993) 3581.
- [19] T. Kato, T. Uryu, *Liq. Cryst.* 14 (5) (1993) 1311.
- [20] D.L. Pavia, G.M. Lampman, G.S. Kriz, *Introduction to Spectroscopy*, third ed., Harcourt College, Boston, 2001; H. Kihara, T. Kato, T. Uryu, J.M.J. Frechet, *Chem. Mater.* 8 (1996) 961.
- [21] M. Srinivasulu, P.V.V. Satyanarayana, P.A. Kumar, V.G.K.M. Pisipati, *Z. Naturforsch. A: Phys. Sci.* 56a (2002) 685.
- [22] P. Swathi, P.A. Kumar, V.G.K.M. Pisipati, A.V. Rajeswari, S. Sreehari Sastry, P. Narayana Murty, *Z. Naturforsch.* 57a (2002) 797.
- [23] E.B. Barmatov, A. Bobrovsky, M.V. Barmatova, V.P. Shibaev, *Liq. Cryst.* 26 (1999) 581.
- [24] P.G. De Gennes, *The Physics of Liquid Crystals*, Oxford Press, London, 1974.
- [25] S. Chandrasekhar, *Liquid Crystals*, Cambridge University Press, New York, 1977.
- [26] H.E. Stanley, *Introduction to Phase Transition and Critical Phenomena*, Clarendon Press, New York, 1971.